
COMPARATIVE ANALYSIS OF AUDIO FEATURE EXTRACTION FOR REAL-TIME TALKING PORTRAIT SYNTHESIS

Pegah Salehi
SimulaMet
Oslo, Norway
pegah@simula.no

Sajad Amouei Sheshkal
SimulaMet
Oslo, Norway
sajad.amouei@gmail.com

Vajira Thambawita
SimulaMet
Oslo, Norway
vajira@simula.no

Sushant Gautam
SimulaMet
Oslo, Norway
sushant@simula.no

Saeed S. Sabet
Forzasys
Oslo, Norway
saeed.sh.sabet@gmail.com

Dag Johansen
The University of Tromsø
Tromsø, Norway
dag.johansen@uit.no

Michael A. Riegler
SimulaMet
Oslo, Norway
michael@simula.no

Pål Halvorsen
SimulaMet
Oslo, Norway
paalh@simula.no

November 21, 2024

ABSTRACT

This paper examines the integration of real-time talking-head generation for interviewer training, focusing on overcoming challenges in Audio Feature Extraction (AFE), which often introduces latency and limits responsiveness in real-time applications. To address these issues, we propose and implement a fully integrated system that replaces conventional AFE models with Open AI’s Whisper, leveraging its encoder to optimize processing and improve overall system efficiency. Our evaluation of two open-source real-time models across three different datasets shows that Whisper not only accelerates processing but also improves specific aspects of rendering quality, resulting in more realistic and responsive talking-head interactions. These advancements make the system a more effective tool for immersive, interactive training applications, expanding the potential of AI-driven avatars in interviewer training.

Keywords Talking Portrait Synthesis, Interactive Avatar, Whisper, Neural Radiance Fields (NeRF), child protective services (CPS)

1 Introduction

The application of AI in education has gained widespread attention for its potential to enhance learning experiences across disciplines, including psychology [1, 2]. In the context of investigative interviewing, especially when questioning suspected child victims, AI offers a promising alternative to traditional training approaches. These conventional methods, often delivered through short workshops, fail to provide the hands-on practice, feedback, and continuous engagement needed for interviewers to master best practices in questioning child victims [3, 4]. Research has shown that while best practices recommend open-ended questions and discourage leading or suggestive queries [5, 6], many interviewers still struggle to implement these techniques effectively during real-world investigations [7]. The adoption of AI-powered child avatars provides a valuable solution, enabling Child Protective Services (CPS) workers to engage in realistic practice sessions without the ethical dilemmas associated with using real children, while simultaneously offering personalized feedback on their performance [8].

Our current system leverages advanced AI techniques within a structured virtual environment to train professionals in investigative interviewing. Specifically, this system integrates the Unity Engine to generate virtual avatars. Despite the potential advantages of our AI-based training system, its effectiveness largely depends on the perceived realism and fidelity of the virtual avatars used in these simulations [9]. Based on our findings, we observed that avatars generated using Generative Adversarial Networks (GANs) demonstrated higher levels of realism compared to those created with the Unity Engine in several key aspects [10].

Accordingly, in this paper, we propose leveraging existing real-time talking portrait generation techniques to create an interactive avatar and evaluate its potential for improving perceived realism and interaction quality.

Audio-driven talking portrait synthesis enables the animation of a specific person based on arbitrary speech input, using deep learning-based methods such as Neural Radiance Fields (NeRF) [11] and 3D Morphable Models (3DMMs) to generate high-quality 3D head models that offer flexibility in head poses and superior visual fidelity. Despite advancements in the development of real-time talking head systems, their broad availability remains constrained by the inherent complexity of integrating multi-modal data inputs, including audio and visual cues such as facial landmarks. This complexity poses challenges in achieving both synchronization and processing efficiency, which are imperative for the smooth operation of these systems in real-time scenarios.

In audio-driven talking-head synthesis, the nuances of audio features directly influence the realism and synchronization of the generated visuals. Since different AFE models capture slightly varied aspects from the same audio stream, selecting the most effective model becomes essential. Through our exploration of open-source real-time talking head models, we observed that latency in AFE can hinder real-time performance, impacting the overall responsiveness and realism of the avatar. To mitigate the latency issues associated with existing Audio Feature Extraction (AFE) models, we have leveraged Whisper [12], an advanced automatic speech recognition (ASR) system that has been adapted for AFE tasks. Trained on extensive multilingual and multitask datasets, Whisper offers an efficient and accelerated solution for AFE, potentially optimizing the real-time capabilities of talking head systems.

In summary, our main contributions are as follows:

- Integrating a complete AI-based avatar system combining GPT-3 for conversations, Speech-To-Text (STT), Text-To-Speech (TTS), AFE, and talking portrait synthesis (Figure 1) for full end-to-end experiments.
- Evaluating and comparing talking-head synthesis models.
- Evaluation and comparison of four AFE models using two open-source talking-head frameworks across three datasets.
- Modifying Whisper for efficient and accelerated AFE in talking portrait systems.
- Assessing and discussing the best combinations of talking portrait synthesis systems and AFE systems.

The code and resources related to this work are available on GitHub [13].

2 Related Work

The development and research of our avatar is touching upon two main areas: virtual avatars for interviewer training and real-time talking portrait synthesis.

2.1 Virtual Avatar for Interview Training

The evolution of child avatar training systems has advanced investigative interviewing techniques, albeit with varying degrees of automation and efficacy. Early systems, such as those developed by Linnæus University and AvBIT Labs [14], primarily utilized prerecorded responses, which constrained interaction dynamics. The LiveSimulation [15] enhanced these methods by allowing interaction with a videotaped child, thereby improving open-ended questioning skills [16]. Empowering Interviewer Training (EIT) [17] introduced more dynamic interactions through a rule-based algorithm that facilitated more effective learning with a virtual child. The ViContact [18] further progressed these methodologies by integrating virtual reality (VR) with automated feedback, thereby enhancing both questioning skills and socio-emotional support.

Building on prior advancements, our previous platform [19] integrated GPT-3 within a Unity framework to simulate child interviews, aiming to improve response dynamism and training effectiveness. Despite these efforts, the system was criticized for the lack of realism in avatar appearance, which detracted from user engagement during interactions [19]. To address this issue, our current work aims to utilize lifelike talking portrait generation in real-world applications, specifically for training in child interview skills, with the expectation that it will improve visual realism.

2.2 Talking Portrait Synthesis

In recent years, real-time audio-driven talking portrait synthesis has garnered significant attention due to its applications in digital humans, virtual avatars, and video conferencing. Several approaches have been proposed to balance visual quality, synchronization, and computational efficiency. Live Speech Portrait [20] uses auto-regressive predictive coding

(APC) [21] for extracting speech information, predicts 3D lip landmarks from audio, and synthesizes video frames through an image-to-image translation network (U-Net). Similarly, RealTalk [22] utilizes 3D facial priors and efficient expression rendering modules to achieve precise lip-speech synchronization while preserving facial identity.

Furthermore, 3D Gaussian Splatting (3DGS) [23] introduces a point-based rendering technique that uses ellipsoidal, anisotropic Gaussians to represent scenes with high accuracy. GSTalker [24] builds on this by incorporating deformable Gaussian splatting, significantly reducing training times and boosting rendering speeds compared to earlier NeRF-based models. Gaussian Talker [25] further advances the field by using a Gaussian-based model to generate talking faces with high-quality lip synchronization while reducing computational complexity.

Moreover, NeRF [11] has recently gained attention for generating talking portraits, given their capacity to capture intricate visual scenes. To enhance system efficiency, RAD-NeRF [26] incorporates discrete learnable grids in AD-NeRF [27], resulting in faster training and inference processes. Building upon this, ER-NeRF [28] utilizes tri-Plane hash representation to minimize hash collisions, leading to faster convergence, while a cross-modal fusion mechanism has been developed to improve lip-speech synchronization. To further refine lip synchronization, GeneFace++ [29] introduces a dedicated audio-to-motion module within the NeRF-based rendering framework. Additionally, R2-Talker [30] employs a progressive multilayer conditioning approach, improving performance and visual fidelity by integrating hash-grid landmark encoding.

3 Methodology

This section introduces the AFE models—Deep-Speech 2, Wav2Vec 2.0, HuBERT, and Whisper—compared in this study and outlines the interactive avatar’s system architecture.

3.1 Audio Feature Extraction

A key aspect of talking-head generation is the ability to capture distinguishing speech features, as this directly affects the synchronization and quality of the audiovisual output. In the proposed framework, feature extraction is conducted using four ASR models: Deep-Speech 2 [31], Wav2Vec 2.0 [32], HuBERT [33], and Whisper [12]. Each of these models extracts both acoustic features and language representations from raw audio signals as part of their architecture. The following sections provide further details on these four models.

3.1.1 Deep-Speech 2

Deep-Speech 2, developed by Baidu, utilizes bidirectional recurrent neural networks (BRNNs) [34] alongside convolutional layers to capture context from both past and future frames, enhancing speech recognition accuracy. Key techniques like Batch Normalization and SortaGrad stabilize training, making the model effective across different acoustic conditions, including noisy environments [31].

3.1.2 Wav2Vec 2.0

Wav2Vec 2.0 is a transformer-based model developed for self-supervised feature extraction directly from raw audio signals [32]. Initially, the model processes audio waveforms into representations using a convolutional neural network (CNN) paired with a Gaussian Error Linear Unit (GELU) activation function [35], which captures latent speech features across temporal frames z_1, z_2, \dots, z_T . These features are then fed into a transformer network [36], which is trained through a contrastive loss objective. This loss function enables the model to differentiate between correct and incorrect quantized representations of the audio signal [37].

This self-supervised training allows Wav2Vec 2.0 to learn rich, contextualized embeddings from unlabeled speech data, effectively building contextual representations across continuous speech and capturing dependencies over the entire sequence of latent representations. This approach reduces the need for hand-engineered features, while leveraging the powerful representations learned by Wav2Vec 2.0, resulting in improved performance for various speech processing applications.

3.1.3 HuBERT

Hidden-Unit BERT (HuBERT) [33] introduces a self-supervised approach that addresses key challenges in speech processing: handling multiple sound units per utterance, the lack of lexicon during pre-training, and the absence of explicit segmentation of sound units. By applying prediction loss to masked regions, HuBERT learns a combined acoustic and language model from unmasked inputs. Pre-trained on Librispeech [38] (960 hours) and Libri-light [39]

(60,000 hours), it outperforms previous methods and comes in three sizes: BASE (90M parameters), LARGE (300M), and X-LARGE (1B). HuBERT employs masking similar to SpanBERT [40] and wav2vec 2.0 [32], using cross-entropy loss on masked and unmasked time steps, encouraging the model to capture both acoustic features and long-range speech patterns.

3.1.4 Whisper

In this paper, we propose the use of Whisper Tiny [12], designed for lightweight applications, offers efficient processing and broad applicability in low-resource or edge environments. With approximately 39 million parameters, it is tailored for real-time applications on less powerful devices while maintaining the core Whisper architecture. This model follows an encoder-decoder Transformer structure, allowing it to perform versatile multilingual transcription, translation, and voice activity detection within a compact and efficient design, making it particularly suitable for talking-head systems and real-time audio-visual synchronization tasks.

Whisper Tiny uses log-Mel spectrograms as input features, derived from 25-millisecond windows with a 10-millisecond stride, which are scaled to a near-zero mean. This spectrogram is processed through Transformer encoder blocks containing convolutional layers with GELU activations [35]. These layers capture critical acoustic and linguistic features across languages and environments, leveraging Whisper’s extensive pre-training on multilingual, multitask datasets. This approach provides the model with robust noise resilience and the ability to maintain high accuracy without dataset-specific fine-tuning.

The Whisper model’s design has demonstrated a substantial 80-90% reduction in processing times compared to alternative models like Deep-Speech, Wav2Vec, and HuBERT, particularly for longer audio clips (see Fig. 3).

The Whisper model processes raw audio $A(t)$ by transforming it into a log-Mel spectrogram $S(f, t)$ as follows:

$$S(f, t) = \log \left(\sum_{k=0}^{N-1} A(t) \cdot e^{-j2\pi ft} \right)$$

This spectrogram, capturing core frequency components, is then passed through Whisper’s encoder to generate high-dimensional audio embeddings E :

$$E = \text{WhisperEncoder}(S(f, t))$$

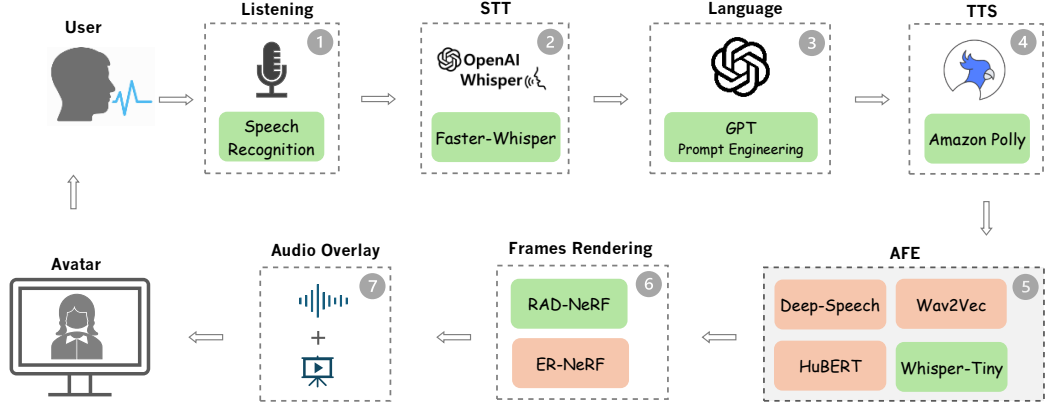
where E has shape (T_{initial}, C) , with T representing the number of time steps aligned to the visual frames, and $C = 384$ as the dimensionality of the feature embedding space. Synchronization with a 25 FPS visual frame rate is achieved by applying a sliding window with parameters $w = 16$, stride $s = 2$, and padding $p = 7$, yielding a final feature matrix with shape $(750, 16, 384)$. This setup ensures precise temporal alignment across 750 frames over 30 seconds, enhancing the real-time accuracy and fluidity of interactions in talking-head applications.

3.2 System Architecture

The system architecture of our interactive child avatar, as depicted in Figure 1, is composed of several modules: Listening, STT, Language, TTS, AFE, Frames Rendering, and Audio Overlay.

The Listening module is the entry point of the system, where user speech is captured through a button-based recording process. Users click to start recording their voice input and click again to stop, saving the recorded audio file. During this recording phase, the avatar remains in a listening state, utilizing a pre-rendered video based on an empty audio file where it exhibits natural, non-verbal behaviors such as blinking and subtle movements while remaining silent. This module employs a speech recognition system to continuously listen for spoken input from the user, initiating the conversion process by passing the audio data to the speech-to-text module.

The STT module utilizes OpenAI’s Whisper model [12] to perform real-time conversion of spoken input into text, transcribing the user’s speech for further processing. The language module is responsible for generating contextually appropriate and dynamic responses. It leverages GPT for prompt engineering, simulating a child’s conversational style. The transcribed text from the STT is processed here, where GPT generates relevant responses tailored to the interaction context. Once the response text is generated, it is passed to the TTS, which uses Amazon Polly [41] to convert the text into speech. This module maintains the consistency of the avatar’s voice with a child’s persona.



(a) Child avatar system architecture



(b) User interacting with the avatar

Figure 1: (a) System architecture of the interactive child avatar, detailing the integration of key modules: (1) Listening, (2) STT, (3) Language Processing, (4) TTS, (5) AFE, (6) Frames Rendering, and (7) Audio Overlay. This setup simulates natural conversation, allowing the user to interact with the avatar as if communicating with a real person. (b) User interaction with the child avatar system.

AFE processes the incoming audio from the TTS module to extract relevant features. To achieve rapid and efficient audio processing that enhances the system’s responsiveness, four models were evaluated: Deep-Speech [31], Wav2Vec [32], HuBERT [33], and Whisper-Tiny [12].

The Frames Rendering module manages the visual representation of the avatar. It is responsible for rendering frames in real-time based on the processed audio and text input, allowing the avatar to exhibit natural behaviors such as lip-syncing and facial expressions synchronized with the spoken output. We also compared two frameworks, RAD-NeRF [26] and ER-NeRF [28], to identify the most effective solution for this purpose. The final component is the Audio Overlay module, which combines the rendered frames with the audio output.

4 Experiments

This section rigorously evaluates various AFE models across two frameworks, focusing on model efficiency, synchronization accuracy, and responsiveness.

4.1 Experimental Setup

Datasets, hardware, and configurations are outlined for evaluating AFE model performance in real-time talking portrait synthesis.

4.1.1 Dataset

The dataset used in our experiments comprises a combination of publicly available video datasets and a privately sourced video. We selected three high-definition speech video clips, each with an average duration of approximately 6,700 frames (around 4.5 minutes, as recorded at 25 FPS). The raw videos, originally recorded at their native resolutions (which can also be used in the experiments), were cropped and resized to 512×512 pixels. However, the Obama video from AD-NeRF [27], which was originally processed at 450×450 pixels, was used in that resolution without further resizing.

To ensure fairness and reproducibility, two of the video clips used in our experiments were sourced from the Internet. Specifically, we utilized the "Obama" video from the publicly released data of AD-NeRF [27] and the "Shaheen" video. The third video clip, featuring a young girl's speech, was privately sourced to align with the application objectives of the investigative interview. Explicit permission was obtained from the individual for the use of this video in this research.

For each video, the first 91% frames, along with the corresponding audio, were used as training data, while the final 9% of the data was reserved for subsequent evaluation, in accordance with previous studies [27, 26, 28].

4.1.2 System Configuration

Experiments were conducted on a machine with a 12th Gen Intel(R) Core(TM) i9-12900F CPU, 31 GiB of RAM, and an NVIDIA RTX 4090 GPU with 24 GiB of VRAM, running CUDA 12.4 on an Ubuntu operating system.

4.2 Real-Time Talking-Head Speed Analysis

Despite progress in real-time talking-head systems, their widespread use is limited by the complexity of integrating multimodal inputs like audio and facial landmarks. This complexity challenges both synchronization and processing efficiency, which are required for smooth real-time performance. Given these challenges, we considered it necessary to evaluate the real-time capabilities of existing models to substantiate performance claims. To accurately assess the efficiency of these models, we conducted an experiment using the Obama dataset [27]. The experiment was carried out under identical hardware and CUDA environments across all applicable open-source methods, ensuring a consistent basis for comparison.

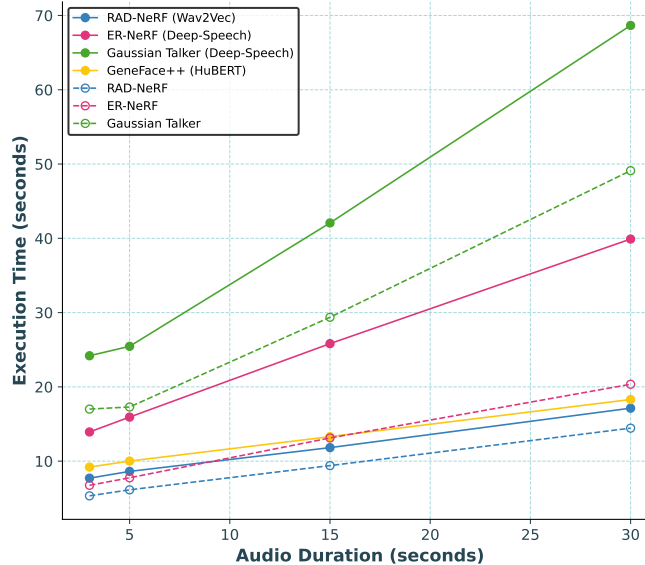


Figure 2: Execution time comparison of open-source real-time talking-head generation models, including RAD-NeRF [26], ER-NeRF [28], Gaussian Talker [25] and GeneFace++ [29]. The solid lines represent execution times excluding AFE, while the dashed lines indicate execution times that include AFE.

Our findings confirm that a major challenge identified in previous studies is the latency introduced during the AFE process. To better understand the impact of AFE on overall system performance, we measured execution time using two different approaches: one excluding AFE and the other including it. GeneFace++ [29] is excluded from this comparison, as its audio features are deeply interwoven within the core of the model, making it impossible to measure

its performance without AFE. The results, presented in Figure 2, illustrate the comparative processing efficiency of these models across different audio durations.

4.3 AFE Analysis

Based on the results presented in Figure 2, we selected RAD-NeRF [26] and ER-NeRF [28] as the frameworks for further experimentation due to their better performance compared to other models. To conduct a systematic comparison of AFE models, we will employ Deep-Speech, Wav2Vec [32], HuBERT [33], and Whisper-Tiny [12] within both RAD-NeRF [26] and ER-NeRF [28]. The models will be trained from scratch with each AFE configuration to assess their impact on system performance, focusing on factors such as lip synchronization accuracy, visual quality, and overall execution time. In the following, we divide the analysis into two key aspects—speed and quality—to provide a more detailed evaluation of each AFE configuration’s impact on system performance.

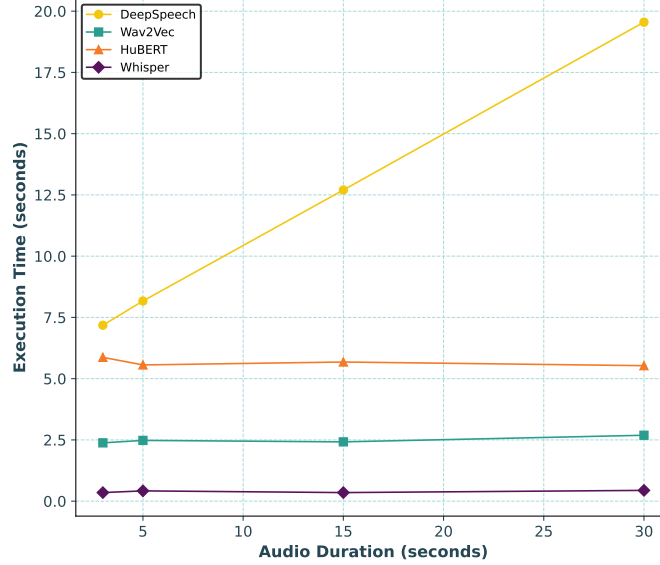


Figure 3: Execution time comparison of different AFE models, including Deep-Speech [31], Wav2Vec [32], HuBERT [33], and Whisper [12].

4.3.1 AFE Speed Analysis

In evaluating the speed of AFEs, we conducted an analysis between Whisper [12] and other well-known AFE models, including Deep-Speech [31], Wav2Vec [32], and HuBERT [33]. The results, illustrated in Figure 3, reveal that Whisper greatly outperforms the other models across varying audio durations, especially compared to Deep-Speech, which shows increasing execution times as audio duration grows. Whisper consistently achieves notably lower execution times, making it particularly advantageous for conversational systems.

Additionally, Figure 4 compares the execution times of RAD-NeRF [26] and ER-NeRF [28] using various AFE models, including Whisper, Deep-Speech [31], Wav2Vec [32], and HuBERT [33]. The results show the time-saving advantages of Whisper across both models. By integrating Whisper, we achieved a reduction in processing time, which is important for real-time applications such as talking-head generation and interactive avatars. These findings reveal the potential of Whisper as an effective solution for accelerating AFE processes in interactive avatar systems, making them more efficient and responsive.

4.3.2 AFE quality Analysis

To further validate utilizing Whisper as AFE, we conducted an evaluation of the system’s rendering quality across various settings. In the self-driven setting, where the ground truth data corresponds to the same identity as the generated output, we employ several quantitative metrics to assess the quality of portrait reconstruction:

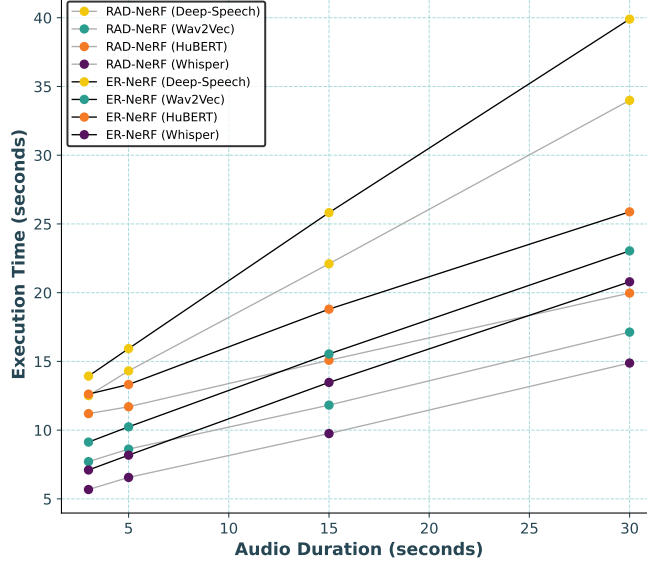


Figure 4: Execution time comparison of RAD-NeRF [26] and ER-NeRF [28] across different AFE models.

- **Peak Signal-to-Noise Ratio (PSNR):** This metric measures the fidelity of the reconstructed image relative to the ground truth. The PSNR is calculated as:

$$\text{PSNR} = 10 \cdot \log_{10} \left(\frac{\text{MAX}_1^2}{\text{MSE}} \right)$$

where MAX_1 is the maximum possible pixel value of the image, and MSE is the Mean Squared Error between the reconstructed and ground truth images.

- **Structural Similarity Index Measure (SSIM):** SSIM evaluates structural similarity by considering luminance, contrast, and structure. The formula is:

$$\text{SSIM}(x, y) = \frac{(2\mu_x\mu_y + C_1)(2\sigma_{xy} + C_2)}{(\mu_x^2 + \mu_y^2 + C_1)(\sigma_x^2 + \sigma_y^2 + C_2)}$$

where μ_x and μ_y are the average intensities, σ_x and σ_y are variances, and σ_{xy} is the covariance between images x and y . C_1 and C_2 are constants for stability.

- **Learned Perceptual Image Patch Similarity (LPIPS) [42]:** Measures perceptual similarity between the generated and ground truth images by calculating the distance between feature representations extracted from a deep neural network. This metric captures differences in visual features that align more closely with human perception than simple pixel-wise comparisons, making it useful for assessing image quality in terms of perceptual fidelity.

$$\text{LPIPS} = \frac{1}{N} \sum_{i=1}^N \|f(x_i^{\text{pred}}) - f(x_i^{\text{truth}})\|_2$$

where $f(x)$ represents the feature representation of image x extracted by a neural network (e.g., AlexNet), x_i^{pred} and x_i^{truth} are the predicted and ground truth images respectively, and N is the number of patches or feature points compared.

- **Landmark Distance (LMD) [43]:** This metric measures the geometric accuracy of facial landmarks by calculating the Euclidean distance between corresponding landmark points in the generated and ground truth images.

$$\text{LMD} = \frac{1}{N} \sum_{i=1}^N \sqrt{(x_i^{\text{pred}} - x_i^{\text{truth}})^2 + (y_i^{\text{pred}} - y_i^{\text{truth}})^2}$$

where $(x_i^{\text{pred}}, y_i^{\text{pred}})$ and $(x_i^{\text{truth}}, y_i^{\text{truth}})$ are the coordinates of the i -th landmark in the predicted and ground truth images, respectively, and N is the total number of landmarks.

- **Fréchet Inception Distance (FID) [44]:** FID assesses the similarity between distributions of real and generated images. The formula is:

$$\text{FID} = \mu_r - \mu_g^2 + \text{Tr}(\Sigma_r + \Sigma_g - 2\sqrt{\Sigma_r \Sigma_g})$$

where μ and Σ represent the mean and covariance of features for real (r) and generated (g) images.

- **Action Units Error (AUE) [45]:** Measures the accuracy of lower facial muscle movements by calculating the squared differences in action unit intensities between the generated and ground truth images. In this study, we specifically evaluate the lower face region, which is relevant for expressions related to speech and emotion.

$$\text{AUE}_{\text{lower}} = \frac{1}{N} \sum_{i=1}^N (AU_i^{\text{pred}} - AU_i^{\text{truth}})^2$$

where AU_i^{pred} and AU_i^{truth} are the intensities of the i -th action unit in the lower face region for the predicted and ground truth data, respectively, and N is the total number of lower face action units evaluated.

- **SyncNet Confidence Score (Sync) [46]:** Measures the lip-sync accuracy by evaluating the alignment between audio and lip movements in generated talking-head videos. This metric utilizes SyncNet, which calculates a confidence score based on the similarity between embeddings of audio and video frames.

$$\text{Sync} = \frac{1}{N} \sum_{i=1}^N \frac{v_i \cdot s_i}{\max(\|v_i\|_2 \cdot \|s_i\|_2, \epsilon)}$$

where v_i and s_i are the embeddings for the i -th video and audio frames, respectively, computed by SyncNet. This formula calculates the cosine similarity between the embeddings, giving a score between 0 and 1 for each frame pair. N is the total number of frame pairs evaluated, and higher average values indicate better lip-sync quality.

The self-driven evaluation results are shown in Table 1, where the utilization of Whisper for AFE leads to a slight improvement in PSNR and LPIPS metrics. Additionally, the FID scores reflect a minor but consistent improvement in the perceptual similarity between generated and real images. However, the most notable improvement is observed in the Sync, which shows better lip synchronization.

In the cross-driven setting, the model generates a talking portrait based on audio clips that do not match the identity of the visual data used during training. To create variation, two different audio clips are selected for each dataset, corresponding to the gender and age of the character. One audio clip is synthetic, generated using Amazon Polly [41], while the other is a natural recording from a real human, allowing for a fair comparison between synthetic and natural speech.

Because ground truth images corresponding to the same identity are absent, identity-specific metrics are not applicable. Therefore, consistent with prior studies [26, 28], we use the identity-agnostic Sync score [46] as the primary metric to evaluate synchronization between audio and lip movements. This approach allows us to effectively measure the model’s performance when direct comparison with ground truth is not feasible.

The cross-driven results, as shown in Table 2, indicate that models utilizing Whisper generally outperform others, particularly in terms of SyncNet scores. However, Whisper’s superior performance is not consistent across all scenarios. While it shows particular strength in handling human voices, its effectiveness diminishes when dealing with bot-generated voices. Specifically, in our experiments, the bot’s voice was generated at a slower pace and interspersed with more pauses. This slower speech setting may have unintentionally benefited other models, which made them perform better relative to Whisper in this context.

Our experimental results reveal that HuBERT consistently underperforms in lip synchronization, with the lowest Sync scores among all the models tested. Given these results, particularly the poor performance in cross-driven settings (e.g.,

Table 1: Quantitative comparison of face reconstruction quality under self-driven synthesis on the same identity’s test set.

Methods	AFE	Dataset	PSNR \uparrow	SSIM \uparrow	LPIPS \downarrow	LMD \downarrow	FID \downarrow	AUE \downarrow	Sync _{conf} \uparrow
RAD-NeRF [26]	Deep-Speech	Obama	27.14	0.9304	0.0738	2.675	31.29	1.995	7.171
		Donya	27.79	0.9045	0.0917	2.750	12.82	1.911	4.720
		Shaheen	30.13	0.9314	0.0697	3.199	33.05	2.837	7.330
		<i>Mean</i>	28.35	0.9221	0.0784	2.874	25.72	2.247	6.407
	HuBERT	Obama	26.58	0.9261	0.0769	2.762	28.78	2.006	0.563
		Donya	28.05	0.9071	0.0868	2.518	14.25	2.511	0.365
		Shaheen	30.45	0.9332	0.0729	3.050	35.96	3.229	0.494
		<i>Mean</i>	28.36	0.9221	0.0788	2.776	26.33	2.582	0.474
	Wav2Vec	Obama	26.59	0.9268	0.0785	2.696	15.15	1.707	6.744
		Donya	27.12	0.8972	0.0845	2.726	24.58	1.531	4.820
		Shaheen	30.08	0.9306	0.0698	3.221	34.77	2.966	7.946
		<i>Mean</i>	27.93	0.9182	0.0776	2.881	24.83	2.068	6.503
	Whisper	Obama	26.10	0.9231	0.0723	2.573	12.67	1.693	7.143
		Donya	28.65	0.9138	0.0844	2.640	26.85	1.504	5.269
		Shaheen	30.05	0.9303	0.0660	3.045	29.44	2.696	8.488
<i>Mean</i>		28.07	0.9224	0.0761	2.826	24.04	1.964	6.966	
ER-NeRF [28]	Deep-Speech	Obama	26.44	0.9339	0.0441	2.561	7.14	1.923	7.201
		Donya	28.91	0.9165	0.0605	2.647	14.59	1.874	4.722
		Shaheen	29.92	0.9267	0.0450	2.900	16.10	2.668	8.215
		<i>Mean</i>	28.16	0.9257	0.0689	2.7932	20.92	2.155	6.712
	HuBERT	Obama	26.30	0.9297	0.0473	2.758	8.33	1.711	0.300
		Donya	24.20	0.7826	0.1255	2.545	49.81	2.284	0.408
		Shaheen	30.45	0.9322	0.0420	2.852	16.56	3.172	0.434
		<i>Mean</i>	26.98	0.8815	0.0716	2.718	24.90	2.389	0.380
	Wav2Vec	Obama	25.59	0.9268	0.0497	2.645	8.83	1.704	6.616
		Donya	24.21	0.7777	0.1509	2.754	68.20	1.730	4.403
		Shaheen	29.81	0.9245	0.0470	3.003	15.59	2.948	7.917
		<i>Mean</i>	26.53	0.8763	0.0825	2.800	30.87	2.127	6.312
	Whisper	Obama	26.30	0.9314	0.0462	2.501	8.06	1.797	7.647
		Donya	27.36	0.9020	0.0641	2.516	14.67	1.852	5.704
		Shaheen	30.20	0.9305	0.0434	2.935	15.61	3.030	8.575
<i>Mean</i>		28.12	0.9213	0.0654	2.7640	19.29	2.226	7.308	

Table 2: Quantitative comparison of audio-lip synchronization under the cross-driven setting.

Methods	AFE	Dataset	Sync _{conf} \uparrow Synthetic	Sync _{conf} \uparrow Natural
RAD-NeRF [26]	Deep-Speech	Obama	6.581	6.489
		Donya	4.208	3.576
		Shaheen	6.319	5.840
		<i>Mean</i>	5.702	5.301
	HuBERT	Obama	5.109	0.548
		Donya	4.750	0.680
		Shaheen	6.670	0.741
		<i>Mean</i>	5.509	0.656
	Wav2Vec	Obama	6.851	7.388
		Donya	4.593	5.017
		Shaheen	6.837	7.303
		<i>Mean</i>	6.093	6.569
Whisper	Obama	6.884	7.137	
	Donya	4.628	5.742	
	Shaheen	6.347	7.052	
	<i>Mean</i>	5.953	6.643	
ER-NeRF [28]	Deep-Speech	Obama	7.306	7.224
		Donya	5.054	4.851
		Shaheen	6.505	6.074
		<i>Mean</i>	6.323	6.050
	HuBERT	Obama	5.542	0.614
		Donya	4.822	0.480
		Shaheen	7.068	0.581
		<i>Mean</i>	5.810	0.558
	Wav2Vec	Obama	7.219	7.428
		Donya	4.115	4.155
		Shaheen	7.145	7.242
		<i>Mean</i>	6.159	6.275
Whisper	Obama	7.399	8.247	
	Donya	4.651	6.486	
	Shaheen	6.148	7.093	
	<i>Mean</i>	6.066	7.275	



Figure 5: Quality comparison: Examples of visualizations of RAD-NeRF [26] under the self-driven setting, based on two frames extracted from each video illustrating typical challenges. Yellow boxes highlight areas of noisy image quality, while red boxes indicate regions with inaccurate lip synchronization.

Sync scores as low as 0.564), HuBERT appears inadequate for applications requiring precise lip-sync. Future work should consider incorporating subjective evaluations to further assess the perceptual quality and user satisfaction, which may provide a more thorough understanding of its limitations.

Furthermore, we compared the subjective quality and lip-sync performance of two models, RAD-NeRF [26] and ER-NeRF [28], shown in Figure 5 and Figure 6, respectively, using four distinct AFEs under self-driven settings. Each model’s output was evaluated against ground truth to assess its accuracy in audio-driven 3D reconstruction and lip-sync fidelity. For a more comprehensive view of the results, please refer to the supplemental video available on our GitHub repository [13].



Figure 6: Quality comparison: Examples of visualizations of ER-NeRF [28] methods under the self-driven setting, based on two frames extracted from each video illustrating typical challenges. Yellow boxes highlight areas of noisy image quality, while red boxes indicate regions with inaccurate lip synchronization.

ER-NeRF and RAD-NeRF demonstrated varying degrees of fidelity across the AFEs, particularly in achieving accurate lip-sync with the audio input. Generally, Whisper achieved the closest approximation to ground truth across both ER-NeRF and RAD-NeRF, exhibiting strong performance in synchronizing lip movements with audio, especially during pronounced lip articulations, such as the wide-open mouth movements observed when pronouncing sounds like "wa." This precise alignment enhances the realism of the output, particularly in sequences requiring dynamic mouth shapes.

Wav2vec and HuBERT provided reasonable approximations but showed slight misalignments in lip-sync. Deep-Speech, while effective, displayed the greatest variance from ground truth, with notable lip-sync discrepancies, indicating less robust performance in these NeRF-based reconstructions.

4.4 System Responsiveness Analysis

Table 3 outlines execution times per component, with the Listening component excluded due to its dependence on user input duration. The analysis is segmented into raw execution time and the percentage contribution of each stage to the overall system latency, providing a granular view of where time is consumed in the process of generating the interactive avatar’s responses.

Table 3: Execution Time Analysis of Each Component in the System Architecture as Depicted in Figure 1. **AA Tokens:** Number of tokens in the avatar’s answer. **AA Duration (sec):** Length of the avatar’s answer in seconds.

AA Tokens	AA Duration (sec)		STT	Language	TTS	AFE	Frame Rendering	Audio Overlay	SUM
1	0.41	Exe. Time (sec)	0.06	0.80	0.22	0.29	4.05	0.14	5.56
		% of Total	1.08%	14.39%	3.96%	5.22%	72.84%	2.52%	100%
8	1.69	Exe. Time (sec)	0.07	0.96	0.33	0.28	4.75	0.16	6.55
		% of Total	1.07%	14.66%	5.04%	4.27%	72.52%	2.44%	100%
14	3.63	Exe. Time (sec)	0.07	2.45	0.44	0.28	5.45	0.14	8.83
		% of Total	0.79%	27.74%	4.98%	3.17%	61.71%	1.59%	100%
21	5.08	Exe. Time (sec)	0.1	2.27	0.44	0.28	5.88	0.17	9.14
		% of Total	1.09%	24.83%	4.81%	3.06%	64.36%	1.86%	100%
30	6.55	Exe. Time (sec)	0.06	2.76	0.49	0.27	6.58	0.15	10.31
		% of Total	0.58%	26.77%	4.75%	2.62%	63.84%	1.45%	100%
39	9.55	Exe. Time (sec)	0.09	1.95	0.78	0.28	7.52	0.18	10.8
		% of Total	0.83%	18.06%	7.22%	2.59%	69.63%	1.67%	100%
50	12.16	Exe. Time (sec)	0.07	2.08	0.55	0.28	8.65	0.18	11.81
		% of Total	0.59%	17.61%	4.66%	2.37%	73.24%	1.52%	100%

To evaluate the system’s responsiveness, we tested various lengths of avatar answers. This approach allowed us to assess how the system handles different interaction complexities, ranging from brief exchanges like "Hi" and "I'm OK" to more extended dialogues, such as "Um... at Jenny’s house, we play a lot. It’s nice there... but, well, I don’t really like talking about the pool. It wasn’t very fun last time". The results indicate that while the overall system performs efficiently, the frame rendering stages are identified as the most time-consuming, due to the computational demands of generating high-quality, real-time visual output that matches the synchronized audio input.

Conversely, the integration of the Whisper model as the AFE component has proven to be much faster than the conventional AFE models. Whisper’s improved processing speed has substantially reduced the time required to extract and synchronize audio features, contributing to an overall faster system performance.

5 Discussion and Future Work

The results support the value of Whisper [12] as a robust and efficient AFE in real-time talking portrait synthesis, especially for applications that require responsiveness. In comparing execution times across AFE models, including Deep-Speech [31], Wav2Vec [32], HuBERT [33], and Whisper [12], it is evident that Whisper consistently achieves lower execution times. This reduction in processing latency is particularly important for real-time applications where delays can disrupt user engagement [19]. The faster response enabled by Whisper allows smoother interactions in applications like interactive avatars, which improves both the user experience and system reliability.

The performance differences among the AFE models are significant, particularly regarding speed. Whisper’s streamlined architecture, which efficiently processes raw audio into high-dimensional feature embeddings, contrasts with more resource-intensive models like Deep-Speech, which tends to slow down with longer audio durations. This efficiency translates directly to reduced system latency, which is important for maintaining the immediacy expected in real-time avatar interactions. While speed is a significant advantage, Whisper also stands out in synchronization accuracy and visual quality, albeit with smaller differences. Higher SyncNet confidence scores for Whisper indicate superior lip-sync accuracy, a key factor for creating lifelike avatars. This precision contributes to system realism, helping to mitigate the uncanny valley effect [47] that can disrupt user immersion in avatar interactions [10].

Whisper excels in speed and is optimized for multilingual, multitask scenarios, efficiently handling diverse audio inputs with minimal latency. Its feature encoding integrates seamlessly with visual frame rendering, ensuring rapid visual adjustments in real-time speech applications. This design provides an edge over other models by maintaining low execution times across audio durations, which is particularly valuable for dynamic avatars requiring consistent, timely responses.

These findings suggest that Whisper can improve the responsiveness and realism of interactive avatars. However, despite Whisper’s efficiency, the overall system still experiences latency due to other computationally intensive components, such as frame rendering. Future work could focus on optimizing these components or utilizing advanced solutions like NVIDIA’s Avatar Cloud Engine (ACE)¹, a suite of technologies that combines generative AI and hardware acceleration specifically for creating realistic digital humans. By leveraging tools like ACE, which use powerful NVIDIA GPUs to accelerate processes like speech recognition, natural language processing, and real-time facial animation, system responsiveness can be further improved. Additionally, conducting broader user studies with professionals in the field could provide a deeper understanding of the system’s impact on practical outcomes, such as user training and engagement. Expanding this research to include real-world evaluations with subjective user feedback will offer valuable insights into perceived realism, usability, and overall user satisfaction. Incorporating user-centric metrics will provide a more comprehensive view of the system’s effectiveness in high-engagement applications, such as investigative interview training. Through these advancements, AI-driven avatars may achieve greater utility and realism, enhancing their role as effective tools in training applications.

6 Conclusion

This study addressed the latency challenges associated with AFE, which has hindered the practical deployment of real-time talking portrait systems in real-world applications. By integrating the Whisper model—a high-performance ASR system—into our framework, we achieved notable reductions in processing delays. These optimizations not only increased the overall responsiveness of the interactive avatars but also improved the accuracy of lip-syncing, making them more applicable for immersive training applications.

Our findings affirm Whisper’s capability to meet real-time demands, particularly in applications requiring responsive interactions and minimal delay. This efficiency is important for training environments such as CPS, where timely and realistic interactions can greatly impact training efficacy. By achieving these improvements, Whisper-integrated systems emerge as promising solutions for a variety of real-time applications, including virtual assistants, remote education, and digital customer service platforms.

References

- [1] Olga Chernikova, Nicole Heitzmann, Matthias Stadler, Doris Holzberger, Tina Seidel, and Frank Fischer. Simulation-based learning in higher education: A meta-analysis. *Review of educational research*, 90(4):499–541, 2020.
- [2] Helen Crompton, Matthew Bernacki, and Jeffrey A Greene. Psychological foundations of emerging technologies for teaching and learning in higher education. *Current Opinion in Psychology*, 36:101–105, 2020.
- [3] Michael E Lamb. Difficulties translating research on forensic interview practices to practitioners: Finding water, leading horses, but can we get them to drink? *American psychologist*, 71(8):710, 2016.
- [4] Martine B Powell. Designing effective training programs for investigative interviewers of children. *Current issues in criminal justice*, 20(2):189–208, 2008.
- [5] Michael E Lamb, Yael Orbach, Irit Hershkowitz, Phillip W Esplin, and Dvora Horowitz. A structured forensic interview protocol improves the quality and informativeness of investigative interviews with children: A review of research using the nichd investigative interview protocol. *Child abuse & neglect*, 31(11-12):1201–1231, 2007.
- [6] Thomas D Lyon. Interviewing children. *Annual review of law and social science*, 10(1):73–89, 2014.
- [7] Michael E Lamb, Deirdre A Brown, Irit Hershkowitz, Yael Orbach, and Phillip W Esplin. *Tell me what happened: Questioning children about abuse*. John Wiley & Sons, 2018.
- [8] Martine B Powell, Sonja P Brubacher, and Gunn Astrid Baugerud. An overview of mock interviews as a training tool for interviewers of children. *Child Abuse & Neglect*, 129:105685, 2022.
- [9] Syed Zohaib Hassan, Pegah Salehi, Ragnhild Klingenberg Røed, Pål Halvorsen, Gunn Astrid Baugerud, Miriam Sinkerd Johnson, Pierre Lison, Michael Riegler, Michael E Lamb, Carsten Griwodz, et al. Towards an ai-driven talking avatar in virtual reality for investigative interviews of children. In *Proceedings of the 2nd Workshop on Games Systems*, pages 9–15, 2022.
- [10] Pegah Salehi, Syed Zohaib Hassan, Saeed Shafiee Sabet, Gunn Astrid Baugerud, Miriam Sinkerd Johnson, Pål Halvorsen, and Michael A Riegler. Is more realistic better? a comparison of game engine and gan-based avatars

¹<https://developer.nvidia.com/ace>

- for investigative interviews of children. In *Proceedings of the 3rd ACM Workshop on Intelligent Cross-Data Analysis and Retrieval*, pages 41–49, 2022.
- [11] Ben Mildenhall, Pratul P Srinivasan, Matthew Tancik, Jonathan T Barron, Ravi Ramamoorthi, and Ren Ng. Nerf: Representing scenes as neural radiance fields for view synthesis. *Communications of the ACM*, 65(1):99–106, 2021.
- [12] Alec Radford, Jong Wook Kim, Tao Xu, Greg Brockman, Christine McLeavey, and Ilya Sutskever. Robust speech recognition via large-scale weak supervision. In *International conference on machine learning*, pages 28492–28518. PMLR, 2023.
- [13] Pegah Salehi. Whisper afe for talking heads generation. <https://github.com/pegahs1993/Whisper-AFE-TalkingHeadsGen>, 2024. [Accessed 15-02-2024].
- [14] Kevin Charles Dalli. Technological acceptance of an avatar based interview training application: The development and technological acceptance study of the avbit application., 2021.
- [15] Ragnhild Kligenberg Røed, Martine B Powell, Michael A Riegler, and Gunn Astrid Baugerud. A field assessment of child abuse investigators’ engagement with a child-avatar to develop interviewing skills. *Child Abuse & Neglect*, 143:106324, 2023.
- [16] Mairi S Benson and Martine B Powell. Evaluation of a comprehensive interactive training system for investigative interviewers of children. *Psychology, public policy, and law*, 21(3):309, 2015.
- [17] F Pompemma. Training in investigative interviews of children: Serious gaming paired with feedback improves interview quality. doctoral dissertation. *Turku: Åbo Akademi University*, 2018.
- [18] Niels Krause, Elsa Gewehr, Hermann Barbe, Marie Merschhemke, Frieda Mensing, Bruno Siegel, Jürgen L Müller, Renate Volbert, Peter Fromberger, Anett Tamm, et al. How to prepare for conversations with children about suspicions of sexual abuse? evaluation of an interactive virtual reality training for student teachers. *Child Abuse & Neglect*, 149:106677, 2024.
- [19] Pegah Salehi, Syed Zohaib Hassan, Gunn Astrid Baugerud, Martine Powell, Miriam S Johnson, Dag Johansen, Saeed Shafiee Sabet, Michael A Riegler, and Pål Halvorsen. A theoretical and empirical analysis of 2d and 3d virtual environments in training for child interview skills. *IEEE Access*, 2024.
- [20] Yuanxun Lu, Jinxiang Chai, and Xun Cao. Live speech portraits: real-time photorealistic talking-head animation. *ACM Transactions on Graphics (ToG)*, 40(6):1–17, 2021.
- [21] Yu-An Chung and James Glass. Generative pre-training for speech with autoregressive predictive coding. In *ICASSP 2020-2020 IEEE International Conference on Acoustics, Speech and Signal Processing (ICASSP)*, pages 3497–3501. IEEE, 2020.
- [22] Xiaozhong Ji, Chuming Lin, Zhonggan Ding, Ying Tai, Jian Yang, Junwei Zhu, Xiaobin Hu, Jiangning Zhang, Donghao Luo, and Chengjie Wang. Realtalk: Real-time and realistic audio-driven face generation with 3d facial prior-guided identity alignment network. *arXiv preprint arXiv:2406.18284*, 2024.
- [23] Bernhard Kerbl, Georgios Kopanas, Thomas Leimkühler, and George Drettakis. 3d gaussian splatting for real-time radiance field rendering. *ACM Trans. Graph.*, 42(4):139–1, 2023.
- [24] Bo Chen, Shoukang Hu, Qi Chen, Chenpeng Du, Ran Yi, Yanmin Qian, and Xie Chen. Gstalker: Real-time audio-driven talking face generation via deformable gaussian splatting. *arXiv preprint arXiv:2404.19040*, 2024.
- [25] Kyusun Cho, Jounghbin Lee, Heeji Yoon, Yeobin Hong, Jaehoon Ko, Sangjun Ahn, and Seungryong Kim. Gaussiantalker: Real-time talking head synthesis with 3d gaussian splatting. In *ACM Multimedia 2024*, 2024.
- [26] Jiayang Tang, Kaisiyuan Wang, Hang Zhou, Xiaokang Chen, Dongliang He, Tianshu Hu, Jingtuo Liu, Gang Zeng, and Jingdong Wang. Real-time neural radiance talking portrait synthesis via audio-spatial decomposition. *arXiv preprint arXiv:2211.12368*, 2022.
- [27] Yudong Guo, Keyu Chen, Sen Liang, Yong-Jin Liu, Hujun Bao, and Juyong Zhang. Ad-nerf: Audio driven neural radiance fields for talking head synthesis. In *Proceedings of the IEEE/CVF international conference on computer vision*, pages 5784–5794, 2021.
- [28] Jiahe Li, Jiawei Zhang, Xiao Bai, Jun Zhou, and Lin Gu. Efficient region-aware neural radiance fields for high-fidelity talking portrait synthesis. In *Proceedings of the IEEE/CVF International Conference on Computer Vision*, pages 7568–7578, 2023.
- [29] Zhenhui Ye, Jinzheng He, Ziyue Jiang, Rongjie Huang, Jiawei Huang, Jinglin Liu, Yi Ren, Xiang Yin, Zejun Ma, and Zhou Zhao. Geneface++: Generalized and stable real-time audio-driven 3d talking face generation. *arXiv preprint arXiv:2305.00787*, 2023.

- [30] Zhiling Ye, LiangGuo Zhang, Dingheng Zeng, Quan Lu, and Ning Jiang. R2-talker: Realistic real-time talking head synthesis with hash grid landmarks encoding and progressive multilayer conditioning. *arXiv preprint arXiv:2312.05572*, 2023.
- [31] Dario Amodei, Sundaram Ananthanarayanan, Rishita Anubhai, Jingliang Bai, Eric Battenberg, Carl Case, Jared Casper, Bryan Catanzaro, Qiang Cheng, Guoliang Chen, et al. Deep speech 2: End-to-end speech recognition in english and mandarin. In *International conference on machine learning*, pages 173–182. PMLR, 2016.
- [32] Alexei Baevski, Yuhao Zhou, Abdelrahman Mohamed, and Michael Auli. wav2vec 2.0: A framework for self-supervised learning of speech representations. *Advances in neural information processing systems*, 33:12449–12460, 2020.
- [33] Wei-Ning Hsu, Yao-Hung Hubert Tsai, Benjamin Bolte, Ruslan Salakhutdinov, and Abdelrahman Mohamed. Hubert: How much can a bad teacher benefit asr pre-training? In *ICASSP 2021-2021 IEEE International Conference on Acoustics, Speech and Signal Processing (ICASSP)*, pages 6533–6537. IEEE, 2021.
- [34] Mike Schuster and Kuldip K Paliwal. Bidirectional recurrent neural networks. *IEEE transactions on Signal Processing*, 45(11):2673–2681, 1997.
- [35] Dan Hendrycks and Kevin Gimpel. Gaussian error linear units (gelus). *arXiv preprint arXiv:1606.08415*, 2016.
- [36] Alexei Baevski, Steffen Schneider, and Michael Auli. vq-wav2vec: Self-supervised learning of discrete speech representations. *arXiv preprint arXiv:1910.05453*, 2019.
- [37] Herve Jegou, Matthijs Douze, and Cordelia Schmid. Product quantization for nearest neighbor search. *IEEE transactions on pattern analysis and machine intelligence*, 33(1):117–128, 2010.
- [38] Vassil Panayotov, Guoguo Chen, Daniel Povey, and Sanjeev Khudanpur. Librispeech: an asr corpus based on public domain audio books. In *2015 IEEE international conference on acoustics, speech and signal processing (ICASSP)*, pages 5206–5210. IEEE, 2015.
- [39] Jacob Kahn, Morgane Riviere, Weiyi Zheng, Evgeny Kharitonov, Qiantong Xu, Pierre-Emmanuel Mazaré, Julien Karadayi, Vitaliy Liptchinsky, Ronan Collobert, Christian Fuegen, et al. Libri-light: A benchmark for asr with limited or no supervision. In *ICASSP 2020-2020 IEEE International Conference on Acoustics, Speech and Signal Processing (ICASSP)*, pages 7669–7673. IEEE, 2020.
- [40] Mandar Joshi, Danqi Chen, Yinhan Liu, Daniel S Weld, Luke Zettlemoyer, and Omer Levy. Spanbert: Improving pre-training by representing and predicting spans. *Transactions of the association for computational linguistics*, 8:64–77, 2020.
- [41] Amazon Web Services. Aws polly. In *Amazon Web Services*, page <https://aws.amazon.com/polly/>. Amazon, 2024. [Accessed 28-09-2024].
- [42] Richard Zhang, Phillip Isola, Alexei A Efros, Eli Shechtman, and Oliver Wang. The unreasonable effectiveness of deep features as a perceptual metric. In *Proceedings of the IEEE conference on computer vision and pattern recognition*, pages 586–595, 2018.
- [43] Lele Chen, Zhiheng Li, Ross K Maddox, Zhiyao Duan, and Chenliang Xu. Lip movements generation at a glance. In *Proceedings of the European conference on computer vision (ECCV)*, pages 520–535, 2018.
- [44] Martin Heusel, Hubert Ramsauer, Thomas Unterthiner, Bernhard Nessler, and Sepp Hochreiter. Gans trained by a two time-scale update rule converge to a local nash equilibrium. *Advances in neural information processing systems*, 30, 2017.
- [45] Tadas Baltrušaitis, Peter Robinson, and Louis-Philippe Morency. Openface: an open source facial behavior analysis toolkit. In *2016 IEEE winter conference on applications of computer vision (WACV)*, pages 1–10. IEEE, 2016.
- [46] Joon Son Chung and Andrew Zisserman. Out of time: automated lip sync in the wild. In *Computer Vision–ACCV 2016 Workshops: ACCV 2016 International Workshops, Taipei, Taiwan, November 20–24, 2016, Revised Selected Papers, Part II 13*, pages 251–263. Springer, 2017.
- [47] Masahiro Mori, Karl F MacDorman, and Norri Kageki. The uncanny valley [from the field]. *IEEE Robotics & automation magazine*, 19(2):98–100, 2012.